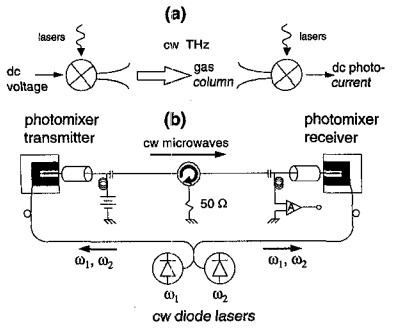

CFB3 Fig. 1. (a) Block diagram for frequency-domain photoconductive sampling. (b) LTG-GaAs photomixers used as transmitter and receiver in proof-of-concept measurements at microwave frequencies (0.05–26.5 GHz).

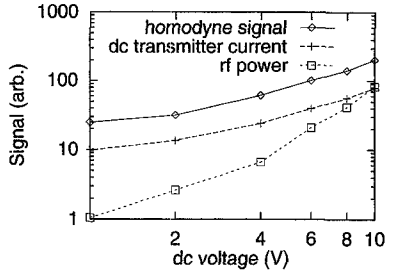

CFB3 Fig. 2. 4.5-GHz homodyne signal detected by the receiver as a function of voltage bias on the transmitter. The coherent signal scales linearly with voltage while the power scales quadratically with voltage. The dc photocurrent in the transmitter is also shown (300 μA at 10 V).

reflector laser diodes is split in half and fiber coupled to each photomixer. Each LTG-GaAs photomixer consists of a 20 μm × 20 μm active region with 0.2-μm-wide interdigitated electrodes spaced by 0.6 μm for the transmitter and by 0.4 μm for the receiver. The transmitter is dc biased through a broadband bias tee and therefore develops an ac current across the electrodes when the photoconductance is modulated at the difference (beat) frequency of the two laser beams. Some of the resulting microwave power is launched onto a coplanar waveguide, which transitions into a 50-Ω coaxial line that is connected in similar fashion to the receiver. At the receiver end, the optical beating periodically raises the photoconductance such that a small amount of unipolar current flows into the dc current amplifier. This action is equivalent to homodyne detection of the rf electric field.

Two experiments have been performed to verify that homodyne detection is occurring. First, the transfer characteristic of a narrow bandpass filter has been measured and agrees with that measured using a microwave spectrum analyzer. Second, as shown in Fig. 2, the homodyne signal scales linearly with the dc-bias voltage (or incident electric field), while the transmitted power measured with a spectrum analyzer scales quadratically. The magnitude of the receiver photocurrent is in good agreement with predictions from a theoretical model that accounts for the impedance mismatch between the photomixers and the transmission line.

Compared to time-domain sampling, the most important advantages of cw photoconductive sampling are spectral brightness and the use of compact inexpensive lasers. The disadvantages include longer acquisition times for measuring very broad spectra and standing waves introduced by the high level of coherence. The latter is why an isolator was used in Fig. 1(b). Also, the frequency resolution depends on the linewidth stability of the laser diodes. Experiments are under way to demonstrate cw sampling at THz frequencies using spiral-antenna coupled photomixers. Such a system, when operational, could be used for many of the "T-ray" applications suggested for time-domain techniques,[4] as well as exotic applications like Doppler processing of signal returns from moving systems.

1. K.A. McIntosh, E.R. Brown, K.B. Nichols, O.B. McMahon, W.F. Dinatale, T.M. Lyszczarz, Appl. Phys. Lett. **67**, 3844 (1995).
2. S. Verghese, K.A. McIntosh, E.R. Brown, IEEE Trans. Microwave Theory Tech. **MTT-45**, 1301 (1997).
3. A.S. Pine, R.D. Suenram, E.R. Brown, K.A. McIntosh, J. Mol. Spectrosc. **175**, 37 (1996).
4. M.C. Nuss, IEEE Circuits Devices Mag. **12**, 25 (1996).

CFB4 (Invited) **8:45 am**

High-power, high-speed, low-temperature-grown GaAs *p-i-n* traveling-wave photodetector

Yi-Jen Chiu, Siegfried B. Fleischer, John E. Bowers, Arthur C. Gossard, Umesh K. Mishra, *Electrical and Computer Engineering Department, University of California at Santa Barbara, Santa Barbara, California 93106; E-mail: chiu@opto.ece.ucsb.edu*

Traveling-wave photodetectors (TWPDs) make it possible to design high-speed detectors with high bandwidth efficiency product.[1–3] The RC time constant limiting the high-speed performance of conventional lumped element photodetectors can be overcome in such TWPD with an impedance matched to the terminating load impedance. Moreover, in a TWPD, the edge-coupled incident light is guided in a waveguide, which is perpendicular to carrier drift direction. The length of the waveguide can thus be chosen to match the absorption length of the light without sacrificing speed. The *p-i-n* absorption region can be optimized for speed while the length of the device is chosen to obtain a high efficiency.

In this work, we successfully fabricated a *p-i-n* TWPD with low-temperature-grown GaAs (LTG-GaAs) as the absorption layer (i-layer). The results show the device performance can be improved by taking advantage of both the short carrier lifetime in the LTG-GaAs and the TWPD structure.[2] Furthermore, we investigated saturation effects in the LTG-GaAs TWPD detector under high optical excitation using electro-optic (EO) sampling. We believe that defect saturation and field screening effects are the main factors determining the saturation energy for higher optical pulse energies.

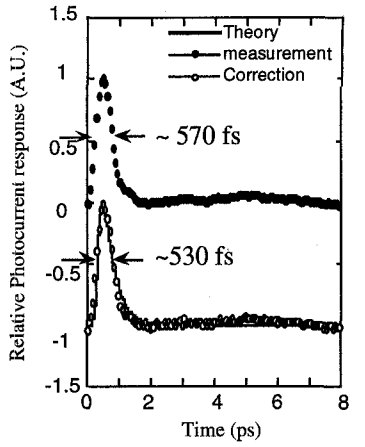

(a)

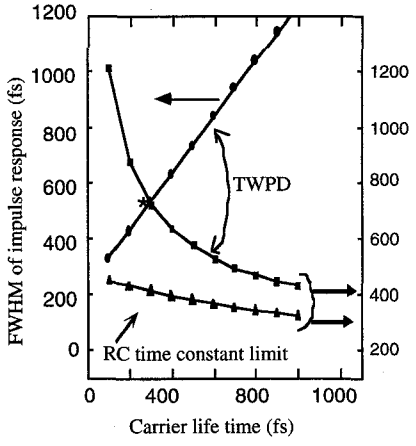

(b)

CFB4 Fig. 1. (a) Normalized electro-optical sampling measurement results. The calculated TWPD pulse response and −3-dB bandwidth with carrier lifetime (b), where '*' is the experiment result (FWHM value).

The material was grown in a molecular beam epitaxy (MBE) system. LTG-GaAs layer (absorption layer 170 nm) was grown at 215°C, and the substrate was subsequently *in situ* annealed at 590°C for 10 min. The *n* and *p* layers (600 nm $Al_{0.2}Ga_{0.8}As$) were deposited at 570°C. The device fabrication followed standard *p-i-n* photodetector processing steps. The material growth and processing are reported in literature.[2]

Pump-probe EO sampling was used to measure the microwave response. Optical pulses of ~150-fs pulse width from an 800-nm mode-locked Ti:sapphire laser were used for the excitation. The optical power level was kept low enough to ensure the device was operated in the linear region. As shown in Fig. 1(a), the FWHM of the measured impulse response is around 570 fs (the corresponding Fourier transform −3-dB bandwidth is 520 GHz). After deconvolving the signal with finite-width optical pulse, the detector response was found to be 530-fs FWHM (560-GHz −3-dB bandwidth). An external dc quantum efficiency of 8% was measured.

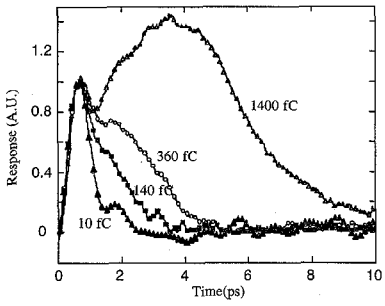

CFB4 **Fig. 2.** Impulse responses at different excitation power with unit fC (photogenerated charge per pulse).

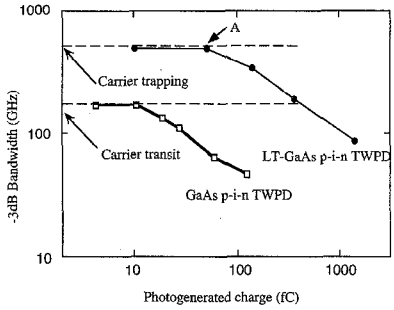

CFB4 **Fig. 3.** Bandwidth at different excitation power.

A simulation was performed to further study the device performance under these low-power (linear) excitation conditions. We assumed that the (distributed) photocurrent was generated along the waveguide as the optical pulse passed. A lossy and dispersive microwave waveguide was considered in the equivalent circuit model. For our calculations, we used device dimensions of 1-μm width, 10-μm length, and 0.17-μm thickness for the LTG-GaAs active region. A 300-fs exponential decay rate was used for the LTG-GaAs carrier lifetime. This 300-fs decay rate was obtained from the transmission pump-probe measurements on samples grown under identical conditions as the LTG-GaAs material used for the fabrication of the detectors. It also agrees with literature values.[4] As shown in Fig. 1(a) (bottom solid line), the theoretical impulse response agrees well with experimental data. Figure 1(b) (right) summarizes the calculated response times of a TWPD as a function of carrier lifetime. For comparison, the RC-imposed bandwidth limit is also shown in the same figure. The response of the fabricated detector is marked with an asterisk in Fig. 1. It is apparent from those traces that the measured low-power response for this detector was mainly dominated by the fast photocarrier trapping in LTG-GaAs.

Figure 2 shows the power dependence of the measured detector response in the linear regime or low excitation (photogenerated charge ~7 fC, ~0.7 W optical peak power). The photocurrent shows a subpicosecond response due to the fast photocarrier trapping in the LTG-GaAs. The optical power was then increased (~140 W peak power or 1400 fC charge/pulse) to study saturation effects in the TWPD. For excitation with high pulse energies, the signal shows an initial fast response similar to the low excitation regime. This fast pulse is then followed by a slower pulse with a few picoseconds duration. As the power increases, the point is reached when all of the traps are filled. This occurs at roughly 60 fC (point A of Fig. 3). The corresponding trap density is around 8×10^{17} cm^{-3}, consistent with the values of Ref. 8. At even higher power levels, the electric-field screening causes a very slow response.[5,6]

To separate the influence of the field screening and trap filling on the device's performance, we compare our results with saturation measurements for GaAs *p-i-n* TWPD[1,6] without the LTG-GaAs active region but otherwise almost identical device parameters. The speed of such devices is limited by the carrier transit time across the absorption layer, and high-power saturation effects are caused by the screening effect only.[6] At low power, these GaAs detectors showed a bandwidth of 170 GHz (effective carrier transit time ~3.5 ps). The bandwidth for the detectors studied here drops below 170 GHz for a photoexcited charge of ~500 fC. This indicates that for higher (>500 fC) excitation levels, the traps are filled, and the detector is now carrier transit time limited. At very high excitations (>500 fC), the device performance becomes limited by field screening.

In summary, we demonstrate a novel type of *p-i-n* photodetectors that incorporates low-temperature-grown GaAs. In the linear regime (low power), the response is very high speed (subpicosecond). At very high excitations, trap filling and charge screening effects degrade the photodetector's performance.

This research is supported by an AFOSR/PRET, Center for Nonstoichiometric III-V Semiconductors under Program No. F49620-95-1-0394.

1. K.S. Giboney, R.L. Nagarajan, T.E. Reynolds, S.T. Allen, R.P. Mirin, M.J.W. Rodwell, J.E. Bowers, IEEE Photonics Technol. Lett. **7,** 412–414 (1995).
2. Y.J. Chiu, S.B. Fleischer, D. Lasaosa, J.E. Bowers, Appl. Phys. Lett. **71** (17), (1997).
3. L.Y. Lin, M.C. Wu, T. Itoh, T.A. Vang, R.E. Muller, D.L. Sivco, A.Y. Cho, IEEE Photonics Technol. Lett. **8,** 1376 (1996).
4. E.R. Brown, K.A. McIntosh, K.B. Nichols, M.J. Manfra, C.L. Dennis, Proc. SPIE **2145,** 200 (1994).
5. A.V. Uskov, J.R. Karin, R. Nagarajan, J.E. Bowers, IEEE J. Sel. Top. Quantum Electron. **1** (1995).
6. K.S. Giboney, M.J.W. Rodwell, J.E. Bowers, IEEE J. Sel. Top. Quantum Electron. **2** (1996).
7. T.S. Sosnowski, T.B. Norris, H.H. Wang, P. Grenier, J.F. Whitaker, C.Y. Sung, Appl. Phys. Lett. **70** (24), (1997).
8. J.P. Ibbetson, U.K. Mishra, Appl. Phys. Lett. **68** (1996).

CFB5 **9:15 am**

Noise reduction in optical pulses and bit-error-rate improvement with a semiconductor-waveguide saturable absorber

H. Yokoyama,* Y. Hashimoto, H. Kurita,
Optoelectronics and High Frequency Device Research Laboratories, NEC Corporation, 34, Miyukigaoka, Tsukuba 305, Japan;
E-mail: yoko@obl.cl.nec.co.jp

The technological development of the Er-doped fiber amplifier (EDFA) dramatically changed the scheme of long-haul optical communications. EDFAs have removed electronic 3R (retiming, reshaping, regeneration) function repeaters. However, although the EDFA provides a regeneration function by an optical method, it also causes the accumulation of spontaneous emission noise during transmission and thus induces communication penalty. Therefore, if an optical noise reduction function is realized using a simple optical method, it will bring a great benefit to optical communication systems. In this paper, we report that the optical noise suppression effect is obtained by using a single-chip semiconductor-waveguide saturable-absorber (SWSA). This device can improve the bit error rate (BER) in high-speed optical communication. This SWSA has a large advantage for real use in a system because of its simple and compact configuration compared to fiber-based interferometer geometries.[1,2]

Figure 1 shows the operation principle of a SWSA and an experimental result of the optical noise pulse suppression. The basic structure of the SWSA is a two-section mode-locked laser diode (MLLD) having a 1.55-μm InGaAsP strained quantum well active layer. The end facets of the device were antireflection coated so that the gain section serves as a traveling-wave amplifier. It was previously

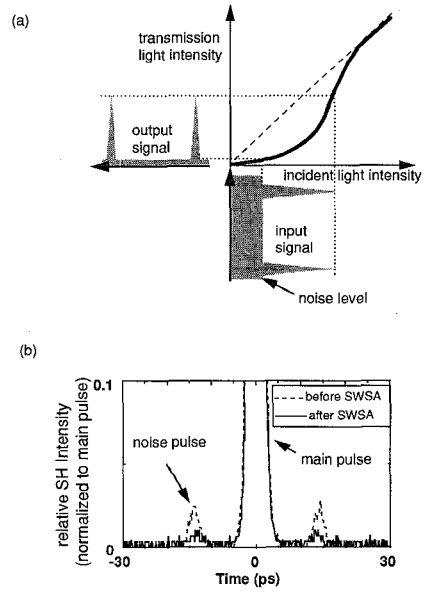

CFB5 **Fig. 1.** (a) Operation principle of a SWSA and (b) SHG intensity correlation traces indicating experimental optical noise pulse suppression.